

Flare Physics in the Hinode Era (Keynote)

David E. McKenzie

*Department of Physics, PO Box 173840, Montana State University,
Bozeman, MT 59717-3840, USA*

Abstract. Hinode's manifest of instrumentation was conceived to investigate the magnetic connections through the photosphere, lower atmosphere, and corona. The complementarity of the instruments is indeed useful, as demonstrated in numerous flares and eruptions in just the first two years of operation. I will review some of the findings from Hinode's observations of flares to date.

It is true, of course, that Hinode's capabilities have evolved since launch. These changes cause the planning of observations to be more complex, and the analysis to be less straightforward; but they do not diminish Hinode's ability to produce important observations of solar flares. On the contrary, Hinode is poised to make truly surprising discoveries. I will explain why this is so, and why we should look forward to the challenge of the coming activity cycle.

1. Introduction

The title of this Keynote Talk covers a very broad topic, and the task is not made easier by the fact that the "Hinode Era" has only barely begun. I will address some possibilities for observing flares with Hinode, giving some examples based on early Hinode results. I will describe what I think should be Hinode's legacy for flare science, based on the same early examples. Finally, I will outline the necessary steps towards fulfilling this goal for Hinode's legacy.

The capabilities of Hinode's instruments are excellently suited for studying flares. SOT produces seeing-free images in $H\alpha$, Ca H, Fe, and G-band; and SOT can make line-of-sight magnetograms, vector magnetograms, and dopplergrams, all with exceptional angular resolution. EIS can make spectra with a very fine slit, or with a variety of wider slots, with high cadence. EIS is sensitive to lines formed over a range of temperatures, in the chromosphere, the transition region, the corona; and can calculate temperatures and densities, doppler and other nonthermal broadening in the emitting plasmas. XRT is designed to image the coronal plasma between approximately one million and twenty million kelvins. With a higher angular resolution than other X-ray telescopes, high sensitivity (and thus fast cadence), and extensive dynamic range, XRT can image the faint plasmas at the same time as brighter emissions. Another major strength of Hinode is that all three instruments are operated jointly and collaboratively. Additionally, the polar orbit allows uninterrupted sunlight for several months at a time; we should not expect to lose sight of a flare because the Earth gets in the way.

There are, of course, some technical and logistical issues which have been discussed elsewhere in this Proceedings. While these issues have to be circum-navigated, Hinode is still an excellent platform from which to do flare science.

2. Early Flare Results: Selected Examples

To demonstrate, I will discuss some examples from flare papers using early Hinode data. Several are based on the intense X-class flares of December 2006; we were indeed very fortunate to be operating at that time.

One paper worth noting is by Asai et al. (2008), in which strong blueshifts were measured with EIS during the X3.4 flare of 13 December 2006. Blueshifts were detected in two features, both of which were observed in the images of XRT. The first feature is identified as a plasmoid ejection, moving across the field of view at a speed of approximately 50 km s^{-1} , with a doppler (line-of-sight) speed of 250 km s^{-1} . This feature appeared at the same time as the first burst of radio emission, suggesting a causal link with the impulsive release of energy, and thereby with the onset of magnetic reconnection in the flare. The second blueshifted feature is a faint arc-shaped ejection, and is similar in appearance to the waves which have been observed with Yohkoh/SXT (Khan & Aurass 2002; Hudson et al. 2003), and SOHO/EIT (Thompson et al. 2000). Asai et al. (2008) suggest this feature may be an MHD fast-mode shock, similar to the findings of Khan & Aurass (2002); Narukage et al. (2002). The observed feature moves along the EIS slit at a speed of 450 km s^{-1} , with a doppler speed of 100 km s^{-1} . This feature has a very broad spectrum, and a temperature of more than 2 million kelvins.

Another paper from the same flare is that by Kubo et al. (2007), concentrating on SOT measurements of the magnetic field before and after the flare. As revealed by the line-of-sight magnetogram in fig.1, the flare occurred along a very convoluted polarity inversion line. Stokes polarization measurements indicate the inclination of the field vector with respect to the line of sight, as well as the azimuth within the plane of the sky; fig.2 shows the azimuth of the field before and after the flare. In this image, white (black) pixels represent magnetic field oriented east-west (north-south). The arrows in fig.2 indicate regions where the field was oriented north-south before the flare; after the flare, the field in those regions appears to have rotated to align with neighboring field, reducing shear.

The paper by Krucker, Hannah, & Lin (2007) combines XRT observations with data from RHESSI to study hard X-ray emission from a loop above the solar limb. This flare was partially over the limb, so the loop's footpoints were obscured, allowing RHESSI to observe the much fainter looptop emission. Some 5 minutes after RHESSI detected hard X-rays, thermal emission from the same loop was observed by XRT. Krucker, Hannah, & Lin (2007) suggest that the electrons were accelerated in the corona, made thin-target emission in the loop, then impacted the chromosphere and evaporated material into the coronal portion of the loop to produce the thermal soft X-ray emission. This interpretation is consistent with the widely accepted model of such flares (McKenzie 2002). The authors inferred an evaporative velocity of approximately 60 km s^{-1} .

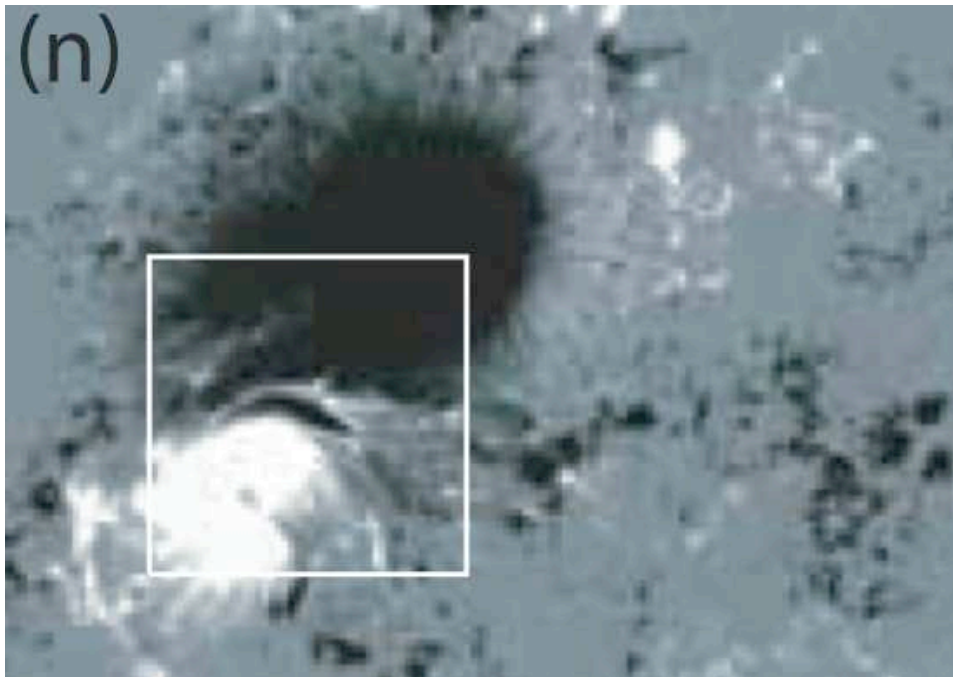


Figure 1. SOT image of longitudinal magnetic field before the 13 December 2006 X3.4 flare. The bright-dark-bright-dark pattern within the box indicates a very convoluted polarity inversion region. Reproduced from Kubo et al. (2007).

Another result is from Jing, Chae, & Wang (2008), again from the 13 December 2006 X-flare. The authors mapped the changing location of the two-ribbon signature during the flare, and superimposed the locations onto a magnetogram of the region to calculate the amount of magnetic flux that was swept over by the ribbons (fig.3). In this way, the authors calculated the reconnection rate as a function of position. They also estimated the localized energy release rate in the same way, by multiplying the square of the magnetic field by the apparent velocity of the ribbons. Jing, Chae, & Wang (2008) found that the peaks in the local reconnection rate, and the sites of maximum energy release, coincided with the locations of the G-band kernels, reinforcing the association of G-band kernels with the site of energy release.

Finally, there is the paper by Reeves, Seaton, & Forbes (2008), demonstrating field line shrinkage in flares. These measurements revisit the analysis by Forbes & Acton (1996), in which the shrinkage of magnetic field lines was estimated as the overall size of the cusp-shaped flaring structure grew. Reeves, Seaton, & Forbes (2008) applied similar techniques to two flares observed by XRT, and found similar shrinkages. The amount of loop shrinkage, and the speed with which the loops contract, are consistent with a prediction from the model by Lin (2004). To remind the reader, the loop shrinkage measured by Forbes & Acton (1996) and by Reeves, Seaton, & Forbes (2008) is determined by identifying a pair of footpoints, and then noting that the field lines connecting those footpoints are initially sharply cusped. While subsequent reconnections

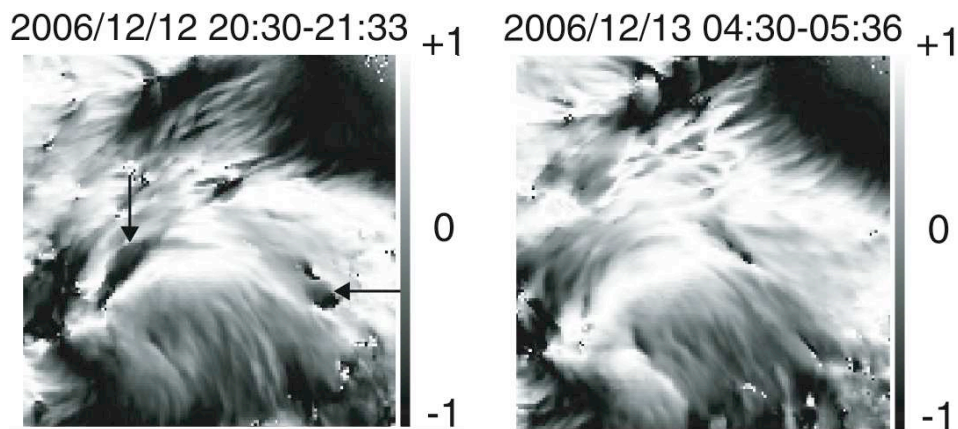


Figure 2. SOT Stokes polarization measurements, showing change in azimuth during the 13 December 2006 X3.4 flare. Black (white) corresponds to field that is oriented north-south (east-west). Reproduced from Kubo et al. (2007).

will add more cusped field lines at greater and greater heights, the initial set of field lines are observed to lose their cusped shape and become more rounded. The reduction of the cusp from the looptops is measured as the loop shrinkage.

Reeves, Seaton, & Forbes (2008) created time-space stackplots by extracting pixels along a slice through the flares' cusps (fig.4). These stackplots demonstrate the shrinkages as faint, downward-sloping traces, and allow a straightforward estimation of the speed. The heights and speeds of the loop shrinkages were compared to the model of Lin (2004), and found to be qualitatively consistent with the model's prediction that field lines closer to the reconnection X-point should shrink faster than those further from the X-point.

3. Defining Hinode's Flare Legacy

Having reviewed Hinode's accomplishments in a few flares, let us now ask the question, "What will be Hinode's legacy for flare science?" To pursue this it is useful to recall, "What was Yohkoh's legacy for flare science?" From the many flares studied by Yohkoh, we know with some certainty that magnetic reconnection is a reality, and plays a vital role in solar flare processes. Of course, Yohkoh did not "invent" reconnection: the articles which outline our standard model for reconnection in eruptive flares predate the mission by many years (Carmichael 1964; Sturrock 1968; Hirayama 1974; Kopp & Pneuman 1976). What Yohkoh contributed was a large number of observations, and comparisons to models, to put the so-called CSHKP model on a firm empirical foundation (McKenzie 2002). Missing from the reconnection picture are some finer details, and I believe this is where Hinode will create its legacy.

For example, we know that reconnection is "patchy", and that patchiness likely arises from some three-dimensional distribution of the plasma resistivity. How shall we understand the localization of the resistivity? What is the source of the resistivity, and what is the cause of the patchiness?

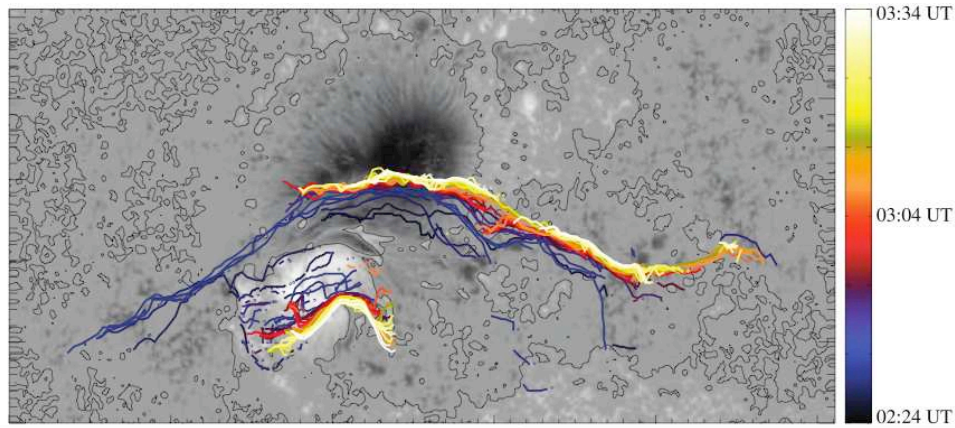


Figure 3. Expansion of two-ribbon signature across the photosphere during the 13 December 2006 X-flare, color-coded to show time evolution. Reproduced from Jing, Chae, & Wang (2008).

Also we notice some pre-flare brightenings in a range of wavelengths, some pre-heating before the impulsive phase of many flares. We do not have a consistent understanding of the cause(s) of such pre-flare brightenings. Are they related to the triggering of the flare? Is pre-flare brightening a signature of early particle acceleration?

We are confident that the energy for a flare is stored in the magnetic field. Our understanding of how the magnetic field is contorted to store this energy is less than perfect, however. Over what time span is the energy stored up? How much does it rely on the rate of helicity injection? And, of course, what triggers the flare? What causes the energy to begin to be released?

The precise mechanism(s) responsible for the acceleration of particles is still uncertain. How important is turbulence in the current sheet for particle acceleration?

How important are the plasmoids and ejecta which are observed in many flares? Are they an after-effect, or are they more closely tied to driving the reconnection, as Shibata (1999) has asserted?

I believe that Hinode's legacy for flare physics should be the answers to these questions. With EIS, SOT, and XRT working together, it is possible to identify the location of flare initiation. We should endeavor to understand which configurations lead to flares, and learn to measure the rate of energy storage. It should be possible to identify inflows and outflows more clearly, and connect them to a better understanding of energy/flux input to the flare, and energy output. Ideally, in the Hinode era we will learn to recognize the location of energy storage, determine the mechanisms of energy/stress buildup, determine the rate of that buildup, determine the time until a threshold is crossed and a flare is triggered, and predict the energy release rate and the fraction of stored energy that will be released.

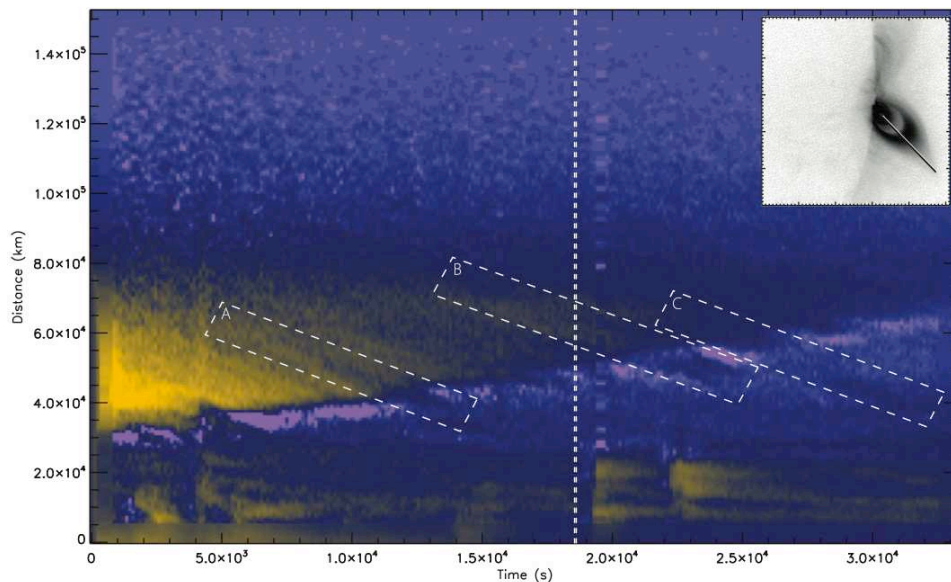


Figure 4. Time-space stackplot of a slice through cuspy flare loops. The shrinkage of field lines is revealed as faint, downward-sloping traces in the stackplot. Reproduced from Reeves, Seaton, & Forbes (2008).

4. Towards Building the Legacy

Returning to the examples from early Hinode flare results, let us consider some possible directions for future study.

The Reeves, Seaton, & Forbes (2008) study of field line shrinkage includes a concise comparison of observation to model, and tentative confirmation that shrinking field lines decelerate after leaving the reconnection X-point. Now, these field line shrinkages are not reconnection outflow, directly; but they are still field lines that are involved in reconnection. With observations it is possible to make quantitative measurements of the reconnection outflows: from the observations of supra-arcade downflows (McKenzie 2000; McKenzie & Savage 2009), there is indication that the outflow speeds are much lower than the Alfvén speed. Might this be due to drag, as suggested by Linton & Longcope (2006), or possibly related to viscosity of the plasma? If the size of a shrinking flux tube is determined by the size of the resistive patch where the reconnection happened (Linton & Longcope 2006), what sizes are observed? How are the resistive patches distributed spatially? Answers to these questions will improve our understanding of the structure of the current sheet and the nature of patchy resistivity. The poster at this meeting by S. Savage (Savage & McKenzie 2009) outlines such observational measurements of the supra-arcade downflows, as well as a model-dependent estimate of the flux contained in each shrinking flux tube (see also McKenzie & Savage 2009).

The Jing, Chae, & Wang (2008) measurements of the local reconnection rate in a two-ribbon flare is a powerful and elegant method for quantifying the energy release. The spatial correlation of reconnection rate with the G-band

kernels supports the idea that reconnection can be enhanced in regions with strong magnetic field. With additional study, can we learn to predict the paths of the ribbons across the photosphere? Doing so would allow prediction of the flux to be included in the flare, and the amount of energy released in the flare.

The Krucker, Hannah, & Lin (2007) article is a demonstration that the observations are consistent with the CSHKP model. It also reveals an opportunity to compare the observations with the model, to improve the model. An example of this type is the poster at this meeting by H. Winter (Winter & Martens 2009). Winter has linked a particle transport code to a hydrodynamic model of coronal loops, to simulate the behavior of loop plasma after the impulsive injection of electrons. By examining the simulated emission from a variety of particle distributions, the investigation illustrates whether the model distributions are consistent with observations.

Recall that in the Kubo et al. (2007) observation, the convoluted polarity inversion line was the site of the relaxation of magnetic shear. The location might have been predictable, based on magnetograms made before the flare (fig.1). Unpredictable, however, were the timing of the flare, the amount of energy to be released, and the amount of shear that would be relaxed. It is hoped that with additional observations of this type, which surely will be acquired in the future, we will learn to identify where the energy is being stored, and at what rate. Can we identify a threshold amount of shear, or a threshold rate of flux collision, as a sign that a flare is imminent?

Asai et al. (2008) interpreted one of the blueshift features as a fast-mode shock. As an impulse propagating through the corona, perturbing the magnetic structures that it encounters, such a shock may be useful as a probe for coronal tomography, or for coronal seismology. To be effective, however, it will be important to know the physical characteristics of the probing shock (e.g., the shock's speed, energy, Mach number). To accomplish this, spectroscopic measurements from EIS must be paired with XRT imaging and SOT magnetograms. Similarly, an understanding of the relationship between the plasmoids and reconnection may require XRT imagery and EIS spectroscopy.

5. Conclusion

The timing of flares in the early phase of the Hinode mission has been fortuitous. Soon after launch and commissioning, a number of large and intense flares were observed with all three instruments. This brief period of activity was followed by many months of relative quiet, during the cycle's activity minimum. This long pause in flare activity has been beneficial, providing time for the team to evaluate the capabilities of the instruments and to make plans to take maximum advantage of Hinode's strengths.

It is true that there are logistical challenges due to telemetry and limits on data capacity. This has always been true, and so the changes after launch and commissioning should not cause undue concern. Because of the issues related to telemetry and the X-band transmitter, all three instrument teams must plan thoughtfully, to coordinate the observations and to produce scientifically useful data without waste. Coordination of the three instruments produces the best science, taking advantage of the complementarity of the instrument capabilities.

The net result of this additional care is an increased probability of acquiring useful data when flaring activity increases in the new cycle.

In a sense, the challenges are also a blessing. Discoveries frequently arrive from unanticipated directions, and often result from using the instrument in ways that the designers did not imagine. With the existing challenges, there are increased opportunities for creative thinking, breaking the expectations upon which the designs were based. In this way, and with increased emphasis on coordination between the three instruments, Hinode is now poised to make fascinating discoveries.

Acknowledgments. The author is supported by subcontract SV7-77003 from Smithsonian Astrophysical Observatory to MSU.

References

- Asai, A., Hara, H., Watanabe, T., Imada, S., Sakao, T., Narukage, N., Culhane, J., & Doschek, G. 2008, *ApJ*, 685, 622
- Carmichael, H. 1964, in *AAS-NASA Symposium on the Physics of Solar Flares*, W. N. Hess, ed., p.451
- Forbes, T.G., & Acton, L.W. 1996, *ApJ*, 459, 330
- Hirayama, T. 1974, *Solar Phys.*, 34, 323
- Hudson, H.S., Khan, J.I., Lemen, J.R., Nitta, N.V., & Uchida, Y. 2003, *Solar Phys.*, 212, 121
- Jing, J., Chae, J., & Wang, H. 2008, *ApJ*, 672, L73
- Khan, J.I., & Aurass, H. 2002, *A&A*, 383, 1018
- Kopp, R. A. & Pneuman, G. W. 1976, *Solar Phys.*, 50, 85
- Kubo, M., Yokoyama, T., Katsukawa, Y., Lites, B., Tsuneta, S., Suematsu, Y., Ichimoto, K., Shimizu, T., Nagata, S., Tarbell, T., Shine, R., Title, A., & Elmore, D. 2007, *PASJ*, 59, S779
- Krucker, S., Hannah, I., & Lin, R. 2007, *ApJ*, 671, L193
- Lin, J. 2004, *Solar Phys.*, 222, 115
- Linton, M., & Longcope, D. W. 2006, *ApJ*, 642, 1177
- McKenzie, D. E. 2000, *Solar Phys.*, 195, 381
- McKenzie, D. E. 2002, in *Multi-Wavelength Observations of Coronal Structure and Dynamics—Proceedings of the Yohkoh 10th Anniversary Meeting*, P.C.H. Martens & D. Cauffman, eds., p.155
- McKenzie, D.E., & Savage, S.L. 2009, *ApJ*, submitted
- Narukage, N., Hudson, H.S., Morimoto, T., Akiyama, S., Kitai, T., Kurokawa, H., & Shibata, K. 2002, *ApJ*, 572, L109
- Reeves, K., Seaton, D., & Forbes, T. 2008, *ApJ*, 675, 868
- Savage, S.L., & McKenzie, D.E. 2009, this Proceedings
- Shibata, K. 1999, *Ap&SS*, 264, 129
- Sturrock, P. A. 1968, in *IAU Symp. 35: Structure and Development of Solar Active Regions*, p.471
- Thompson, B.J., Reynolds, B., Aurass, H., Gopalswamy, N., Gurman, J.B., Hudson, H.S., Martin, S.F., & St. Cyr, O.C. 2000, *Solar Phys.*, 193, 161
- Winter, H.D., & Martens, P. 2009, this Proceedings